The Journal of Neuroscience, November 15, 2000, *20*(22):8629–8636

A Series of Biotinylated Tracers Distinguishes Three Types of Gap Junction in Retina

Stephen L. Mills and Stephen C. Massey

Department of Ophthalmology and Visual Science, University of Texas at Houston, Health Science Center, Houston, Texas 77030

Gap junctions serve many important roles in various tissues, but their abundance and diversity in neurons is only beginning to be understood. The tracer Neurobiotin has revealed many different networks interconnected by gap junctions in retina. We compared the relative permeabilities of five different retinal gap junctions by measuring their permeabilities to a series of structurally related tracers. When large tracers were injected, the staining of coupled cells fell off more rapidly in some networks than others relative to Neurobiotin controls. Three distinctly different permeability profiles were found, suggesting that multiple neuronal connexin types were present. The most permeant to large molecules were gap junctions from A-type horizontal cells. The permeability of gap junctions of two types of amacrine cell were not distinguishable from those from B-type horizontal cells. The lowest permeability was found for gap junctions between cone bipolar cells and the AII amacrine cells to which they are coupled. Because only a single neural connexin type has been identified in retina, our results suggest more types remain to be found.

To determine whether the unitary permeability of channels is altered by channel modulators, we reduced permeability with octanol and a cAMP analog. Although net permeability was substantially diminished, the proportion by which it declined was constant across tracer size. This suggests that these agents act only to close channels rather than alter individual channel permeabilities. This tracer series can therefore be used to contrast permeability properties of gap junctions in intact circuits, even at the level of individual channels.

Key words: gap junction; connexin; tracer coupling; retina; Neurobiotin; metabolic coupling

The conductance and gating properties of many connexin types have been characterized in various expression systems, but only one or two neural connexins have been identified. The properties of neural connexins are therefore poorly characterized, especially in the intact circuits in which they perform their function. This study introduces a series of tracer molecules that can distinguish average channel permeabilities at different sites in intact networks. We provide evidence that at least three different unitary permeabilities are represented in five different gap junctional networks in the mammalian retina.

The use of a tracer series allows us to make two types of comparisons that have been relatively little studied: the permeability of channels to large molecules (Swenson et al., 1989; Bevans et al., 1998; Cao et al., 1998) and the relative permeabilities of gap junctions across different cell types. A single tracer cannot discriminate between permeability differences because of the presence of channels with different unitary permeabilities versus an overall increase in the mean number of open channels of a single type. When additional tracers are used, the ratio of their permeabilities can control for differences in permeability as a result of differences in numbers of open channels of a single type, because the ratio should not change.

Gap junctional permeability is a function of at least size, charge, and reactivity. It is often unclear whether failure to pass a dye is attributable to size or charge differences. Mills and Massey (1995) provided evidence for charge selectivity by finding that biotin-X cadaverine (BXC) (442 Da; +1) will pass gap junctions impermeant to Lucifer yellow (443 Da; −2). Pioneering studies that probed the size of gap junctional channels often used large but dissimilar fluorescent dyes (Brink and Dewey, 1978, 1980; Flagg-Newton et al., 1979; Schwarzmann et al., 1981; Zimmerman and Rose, 1985; Iminaga, 1989; Veenstra et al., 1995) but were able to estimate an effective pore radius. Here, we used a homologous series of cationic tracers from 286 to 555 Da, beginning with Neurobiotin (biotin ethylenediamine). We extended the length of the carbon(yl) spacers between the biotin moiety and the terminal amino group. Each tracer contains a biotin moiety linked to a polyamine, either ethylenediamine or cadaverine. The polyamine is separated from the biotin moiety by zero to two lengths of a hexanoyl spacer (X). Thus, the six molecules are called biotin, biotin-X, or biotin-XX ethylenediamine or cadaverine (Fig. 1).

The molecular and biophysical properties of neuronal connexins are only beginning to be characterized (O'Brien et al., 1996; Condorelli et al., 1998; Srinivas et al., 1999), but the retina has long proven to be a useful tissue for examining neural gap junctions *in vivo* (Vaney, 1999) because of its ease of access and maintenance and variety of gap junctional mosaics. We used our series to characterize four gap junctional networks from rabbit retina by their relative permeability to these tracers. The results suggest variation in gap junctional properties beyond that possible with only the single connexin type thus characterized.

MATERIALS AND METHODS

Individual neurons from isolated rabbit retina labeled with 4,6-diamino-2-phenylindole (DAPI) (Mills and Massey, 1994) or Nuclear yellow (Vaney, 1991) were filled by iontophoresis (+1 nA, 3 Hz) with 4% tracer. A- and B-type horizontal cells were filled continuously for 15 min and then fixed immediately (4% paraformaldehyde, 1 hr). Other cell types were filled for 5 min and then fixed after at least 15 min of diffusion time. The duration of diffusion was recorded for each cell and was used in calculating a rate constant. After tissue fixation, cells were visualized with 1:200 streptavidin-Cy3 (Jackson ImmunoResearch, West Grove, PA).

DAPI and all tracers were obtained from Molecular Probes (Eugene, OR), who also made biotin-XX cadaverine (BXXC) and biotin-XX ethylenediamine by custom synthesis. Junctional permeabilities were lowered by bath application of octanol (Sigma, St. Louis, MO) and Sp-8-CPT-cAMPS (Biolog, La Jolla, CA). Nuclear yellow was obtained from Sigma.

Detection efficiency. To determine the effect of arm length on detection efficiency in our system, we dissolved tracers in 0.2 M PBS and then added

Received June 16, 2000; revised Aug. 18, 2000; accepted Aug. 31, 2000.

This research was supported by National Institutes of Health Grants EY10121 (to S.L.M.) and EY65015 (to S.C.M.) and Core Grant EY10608, and Research to Prevent Blindness (an unrestricted award to the Department of Ophthalmology and Visual Science and the Dolly Green Special Scholar Award to S.L.M.). We thank Alice Chuang for statistical assistance.

Correspondence should be addressed to Stephen Mills, Department of Ophthalmology and Visual Science, University of Texas at Houston, Health Science Center, 6431 Fannin, Room 7.024, Houston, TX 77030. E-mail: smills@eye.med.uth.tmc.edu.

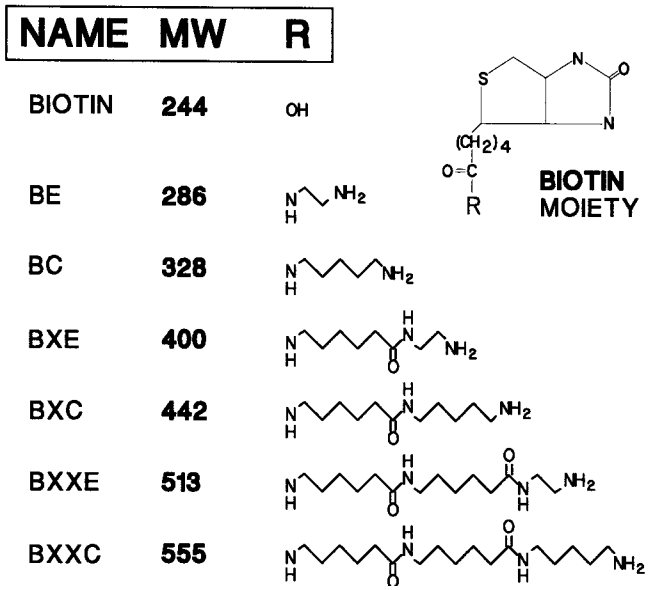

Figure 1. Structures and molecular weights of biotin and the series of tracers constructed from it. *BE*, Biotin ethylenediamine (Neurobiotin); *BC*, biotin cadaverine; *BXE*, biotin-X ethylenediamine; *BXC*, biotin-X cadaverine; *BXXE*, biotin-XX ethylenediamine; *BXXC*, biotin-XX cadaverine; *R*, functional group.

an equal volume of 10% gelatin. Aliquots were blotted onto nitrocellulose paper, fixed in 4% paraformaldehyde for 1 hr, rinsed, and visualized with 1:200 streptavidin-Cy3, following our normal tissue protocols. We used a confocal microscope (LSM-410; Zeiss, Oberkochen, Germany) to measure the fluorescent intensity of each tracer over 5 $\log_{10}$ units of concentration.

Measurement of tracer flux. The rate of movement of tracer across gap junctions is proportional to the magnitude of the concentration gradient and the overall permeability of the array of connexons that form the gap junction. Brightness calibrations and rate coefficients were calculated as described previously (Zimmerman and Rose, 1985; Mills and Massey, 1998), assuming a passive diffusion model with coefficients for delivery rate and junctional permeability. It was assumed that tracer flux across gap junctions was small compared with movement throughout the cell. Lucifer yellow, for example, diffuses throughout an A-type horizontal cell in a few seconds, whereas diffusion into its coupled neighbors requires a minimum of ~1 min. Because A-type horizontal cells have the largest junctional permeability, the ratio of intracellular/junctional fluxes must be even greater in other cell types.

Injection of tracer into AII amacrine cells labels both other AII amacrine cells and ON cone bipolar cells, producing more complex staining patterns than in arrays containing only cells of a single type. Separate coupling rates were calculated for the AII amacrine cell–ON cone bipolar cell pathway and the AII–AII amacrine cell pathway. The equation below illustrates how the rate of change of tracer concentration (C_{Ai}) in a given AII amacrine cell is governed by the concentration gradients to neighboring AII amacrine cells and their associated coupling constant, k_1, and to the ON cone bipolar cell compartments (C_{Bi}) to which it is also coupled and their rate constant, k_2. The differential equation for tracer flux in the bipolar cell simplifies to the rate constant k_2 times the concentration difference for the AII amacrine cell that feeds it. More complicated arrangements, such as including neighboring AII amacrine cells that potentially contact a bipolar cell, did not improve the model.

$$\frac{dC_{A(i)}}{dt} = k_1 * (C_{A(i-1)} + C_{A(i+1)} - 2C_{A(i)}) - k_2 * C_{B(i)}$$

In practice, the coupling rate between AII amacrine cells was estimated as described for simpler arrays; that is, the decline in slope with distance from the injected cell was fit by appropriate choice of k_1. Next, the coupling rate from AII amacrine cells to ON cone bipolars was estimated by choosing the second rate parameter to match the ratio of the intensity of the bipolar cell mosaic relative to the AII amacrine cells (Mills and Massey, 1995). Some iterative adjustment of the two parameters led to the best joint fit.

Retinal neurons are spaced with a wide range of different densities; the density also varies with retinal location within each subtype. It is therefore not meaningful to compare coupling rates based on absolute distance. Distances were normalized by density, so that calculated coupling rates are expressed in number of cells traversed per second rather than centimeters per second. The probability and area of gap junctional contacts is likely to be correlated with distance between cells, but within a regular mosaic of a single type, this will tend to some average value. The regular decline in staining intensity with distance from injected cells seen in our data supports this model. When comparing across cell types with different densities, the overall gap junctional area will of course be different based on spacing and dendritic geometry. This is one of the mechanisms determining overall permeability, along with mean open time and individual channel permeability.

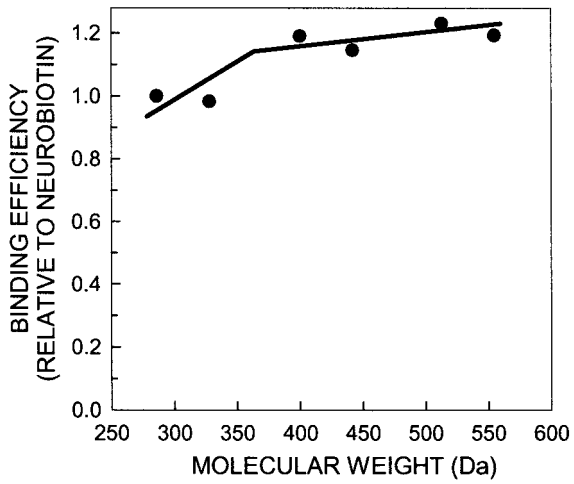

Figure 2. The fluorescent intensity of the tracers in cellulose blots of tracer–serum albumin conjugates after incubation in 1:200 streptavidin-Cy3. Fluorescence was directly proportional to concentration. The smaller tracers bound streptavidin-Cy3 slightly less well than larger tracers.

Distinguishing different unitary permeabilities. Total permeability between two cells is the product of the number of open channels and the average single channel permeability. Suppose two sets of cells are interconnected by gap junctions containing channels of identical type, as if there were only a single type of connexin with a single open conductance state. Then, differences in total permeability to a given tracer would reflect only differences in the number of open connexons. Although the rate of diffusion across the gap junctions would decline with larger tracers, the proportion by which it decreased would be the same for both cell types, regardless of the choice of tracer.

If more than one type of connexin or more than one conductance state is present, however, the connexons can selectively favor passage of one tracer over another. Channels with a small pore diameter will select against larger diameter tracers (Swenson et al., 1989; Werner et al., 1989; Bruzzone et al., 1994). The tracer series can therefore be used to discriminate connexon permeabilities in different cell types, or cells of the same type under different conditions, by injecting different members of the tracer series into coupled networks and comparing the rate at which permeability declines with tracer size.

The coupling rates of the different tracers in the series across the different gap junctions were calculated and normalized relative to Neurobiotin, producing a profile for each gap junctional type relating size of permeant molecules to permeability. Gap junctions consisting of connexons of a single type and measured under comparable conditions should produce identical profiles. Differences in decline with increasing tracer size must reflect differences in permeability of the channels at the two sites.

RESULTS

Detection efficiency

We compared detection efficiencies of the molecules to streptavidin-Cy3, averaged across three binding experiments, and then normalized relative to Neurobiotin. Detection efficiencies were similar across the series (Fig. 2), although the two lightest molecules were ~20% less effective in binding streptavidin-Cy3. For each spacer length, the cadaverine series appeared an average of 8% less effective in binding than the corresponding ethylenediamine tracer, but the only significant differences were between the two lightest tracers and the remaining four.

Iontophoresis, tracer coupling, and reactivity

All of the tracers in this series proved suitable for iontophoresis into neurons. Figures 3 and 4 show examples of A-type (3*A*,*B*) and B-type horizontal cells (4*A*,*B*) stained after injection of Neurobiotin (3*A*, 4*A*) or biotin-XX cadaverine (3*B*, 4*B–D*) into a single cell each. A-type horizontal cells are frequently elongated in rabbit (Fig. 3*C*) and lacking an axon. The characteristic morphology of

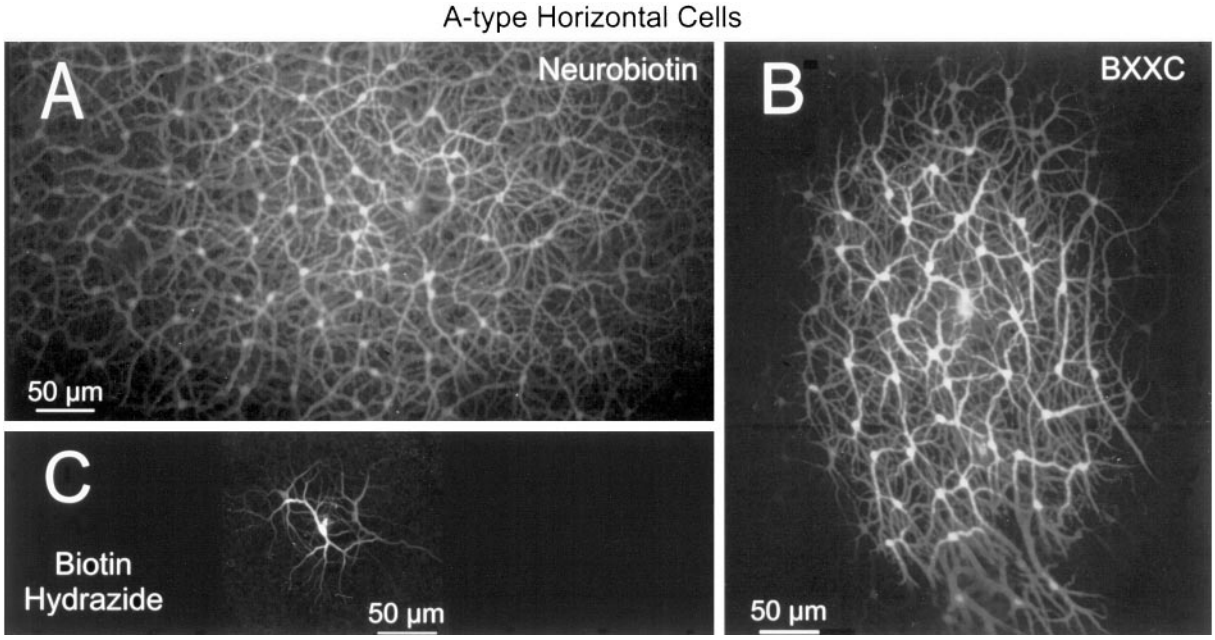

Figure 3. Sample injections of biotinylated tracers into A-type horizontal cells. *A*, Neurobiotin injection produced extensive coupling. *B*, Biotin-XX cadaverine injection produced more concentrated patches. *C*, Biotin hydrazide, the smallest but most reactive tracer, produced little or no coupling.

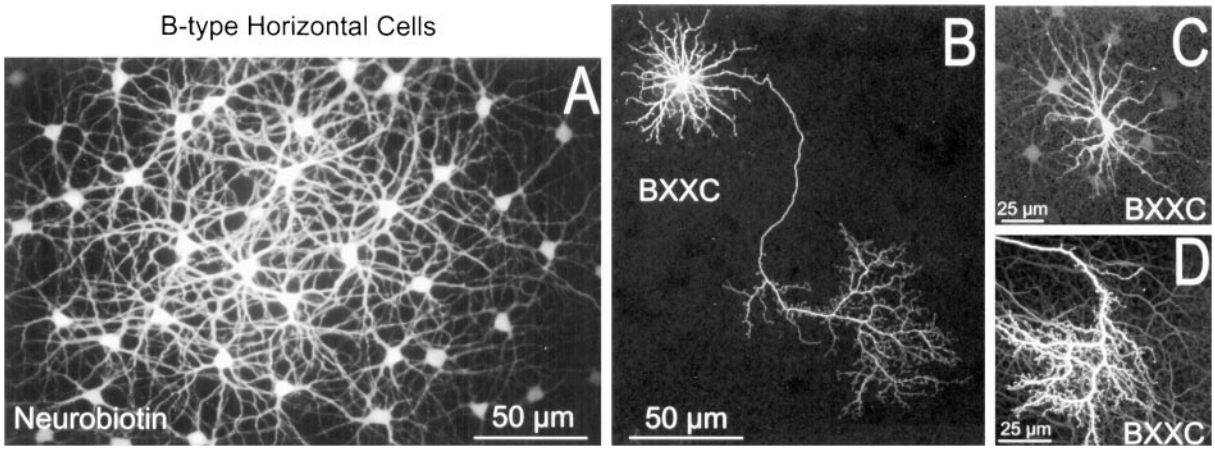

Figure 4. Sample injections of tracer into B-type horizontal cells. *A*, Injection of Neurobiotin led to larger patches (*A*) than corresponding injections of biotin-XX cadaverine (*B–D*). BXXC typically stained 0 (*B*) to 10 (*C*) additional cells but stained the axon terminal more completely (*B*, *D*) than did Neurobiotin. Tracer coupling through gap junctions of the axon terminal was frequently observed (*D*).

B-type horizontal cells is a round soma with many radiate dendrites and a long axon with a large terminal arbor and can be clearly seen in Figure 4*B* because of the lack of significant coupling with BXXC. Neurobiotin injection poorly stains these axons and arbors (Fig. 4*A*) because of the lower impedance pathway through the gap junctions. In each case, far fewer cells were labeled with BXXC (555 Da) than with Neurobiotin (286 Da). Proportionately, however, the decline in coupling with BXXC is much more dramatic for B-type horizontal cells than for the A-type. The number of B-type horizontal cells coupled after BXXC injection varied from none (Fig. 4*B*) to fewer than 10 (Fig. 4*C*) compared with 25–100 with Neurobiotin. In contrast, several hundred A-type horizontal cells are often stained with Neurobiotin, declining ~40% with BXXC.

Tracers with different reactive groups provided clear evidence that reactivity is also an important determinant of tracer flux. Biotin hydrazide, although the smallest tracer used [molecular weight (MW) of 258], was very poorly permeant. This was probably attributable to greater reactivity with proteins, so that the tracer is retained within the injected cell. Contrast the coupling between A-type horizontal cells, which contain the most permissive gap junctions in the retina, with biotin hydrazide (Fig. 3*C*) and longer biotinylated tracers (Fig. 3*A*, Neurobiotin, *B*, BXXC). Injection of many A-type horizontal cells with biotin hydrazide invariably led to few or no detectable biotin hydrazide-coupled cells compared with 25–100 Lucifer yellow-coupled cells or hundreds labeled with Neurobiotin in other locations. No coupling between B-type horizontal cells was ever seen with biotin hydrazide. This suggests that hydrazides are of limited use as tracers, which must be designed for minimum reactivity.

Distinguishing different unitary permeabilities quantitatively

The gap junctions of A- and B-type horizontal cells of rabbit retina are suspected to be different, because the A-type will pass Lucifer yellow readily, whereas the B-type will not (Dacheux and Raviola, 1982; Mills and Massey, 1994). The connexin types have not yet been identified, but use of the tracer series indicates that their functional pore sizes are indeed different. Although qualitative differences in coupling may be seen in Figures 3 and 4, the stronger

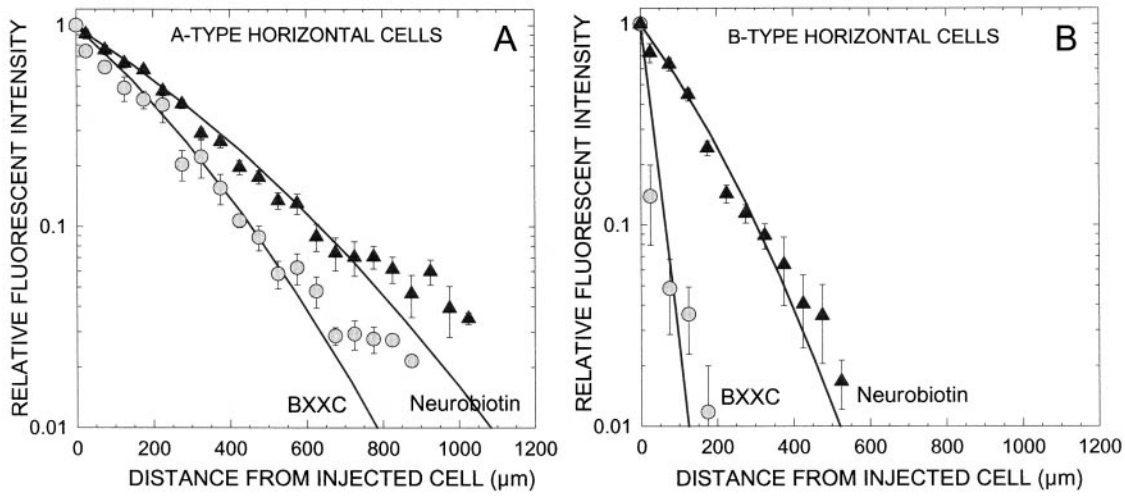

Figure 5. The fluorescent intensity declined as a function of distance from the injected cell and with increasing tracer size (BXXC, 555 Da; Neurobiotin, 286 Da). The decline with larger tracers occurred much more rapidly in B-type horizontal cells (*B*) than in the A-type (*A*).

decline in coupling with larger tracers in B-type horizontal cells is shown more quantitatively in Figure 5. Each *point* is the average of several mosaics of A- or B-type horizontal cells, one each of which was injected with Neurobiotin or BXXC. The rate of decline from Neurobiotin to BXXC is much greater in B-type horizontal cells (Fig. 5*B*) than in A-type horizontal cells (Fig. 5*A*). This clearly indicates that the individual channels in B-type horizontal cells must be less permeant to large molecules than those in A-type horizontal cells. Mills and Massey (1998) estimated the relative permeability of A-type/B-type horizontal cells to be ~19, comparable with receptive field ratios that would reflect electrical coupling (Bloomfield et al., 1995). Differences in number of open channels versus individual channel permeabilities could not be estimated, however. The differences found by Mills and Massey (1998) and this paper were not sufficient to account for failures in Lucifer yellow coupling in B-type horizontal cells. This was despite injecting Lucifer yellow after pharmacological manipulations that approximately equate the amount of tracer flux in A- and B-type horizontal cells when biotinylated tracers are used and also raise the detectability of Lucifer yellow. We therefore conclude that there is an absolute charge barrier to the anionic tracer Lucifer yellow in B-type horizontal cells.

Coupling in a heterologous network

Figure 6*A* shows coupling between members of the AII amacrine cell mosaic (large gray somas); Figure 6*B* shows tracer movement from the AII amacrine cells to the four to five types of ON cone bipolar cell (smaller and sometimes brighter) to which they are also coupled (Vaney, 1991; Mills and Massey, 1995). Biotin-X cadaverine was the tracer. For quantitative comparison, Figure 6*C* shows the intensity profile for a patch of Neurobiotin-coupled AII amacrine cells and for the ON cone bipolar cells coupled to them. Figure 6*D* shows a comparable profile for BXXC. In each case, the *lines* are predictions from the diffusion model, estimated as described in Materials and Methods and by Mills and Massey (1998). When Neurobiotin was injected (Fig. 6*C*), the brightest bipolar cells were of comparable intensity with the amacrine cells; they could even exceed them at certain time intervals because of the dynamics of tracer movement (Mills and Massey, 1995). With BXXC (Fig. 6*D*), the decline in staining in coupled amacrine cells occurred much more quickly.

Coupling to bipolar cells was even more diminished; usually only a few faint bipolar cells were seen near the injected cell. Note that reduced coupling to bipolar cells is seen as a downward translation in these logarithmic plots compared with a change in slope in the horizontal cell plots (Fig. 5). This is because dye transfer to bipolar cells occurs directly from the neighboring amacrine cells at all distances from the injected cell and reflects movement through only a single gap junction, whereas tracer in a distant horizontal cell must have traversed many gap junctions. Hence, the downward translation of bipolar cells occurs because tracer must first move to nearby AII amacrine cells via the kinetics described by the k_1 pathway, which then flows into the bipolar cells at the rate determined by k_2. A measure of the decline in coupling to the bipolar cells can be made without reference to calculated rate constants. Inspection of the data plots shows that the brightest bipolar cells are an average of ~50% as bright as nearby AII cells when Neurobiotin (Fig. 6*B*) was the tracer but only 20% as bright with BXC (Mills and Massey, 1995) and 1% with BXXC (Fig. 6*C*).

How many distinguishably different gap junctional permeabilities are there in retinal neurons?

We have used the tracer series to systematically compare permeability profiles of different gap junctions in a total of four retinal mosaics, one of which contains two separate gap junctional pathways. In each case, the permeability of different coupled retinal cell types was estimated after injection of tracers into cells of that type, and the ratio relative to Neurobiotin was calculated. Figure 7*A* shows that the decline in permeability with increasing tracer size was smallest for A-type horizontal cells but comparable for coupling between B-type horizontal cells and between pairs of amacrine cells. An even more rapid decline with increased tracer size was found in movement of tracer between AII amacrine cells and the ON bipolar cells to which they are coupled. The amacrine cell types represented are the already-noted AII–AII pathway and another well characterized amacrine cell subtype, called S1, which is coupled to neighboring S1 amacrine cells. S1 amacrine cells are wide-field GABA-containing amacrine cells that provide reciprocal inhibitory feedback onto rod bipolar cells (Strettoi et al., 1990). Injection of Neurobiotin into S1 amacrine cells strongly stains as many as 140 neighboring S1 amacrine cells (J. Zhang, W. Li, S. C. Massey, unpublished observations). The ratio of BXXC/Neurobiotin for S1 cells is comparable with that for AII–AII amacrine cell gap junctions and for B-type horizontal cell gap junctions. Although S1 amacrine cells were tested with only two tracers and a small number of injections, and therefore had little statistical power, it is still illustrative to see that another amacrine cell type has a similar permeability profile to those in the intermediate range.

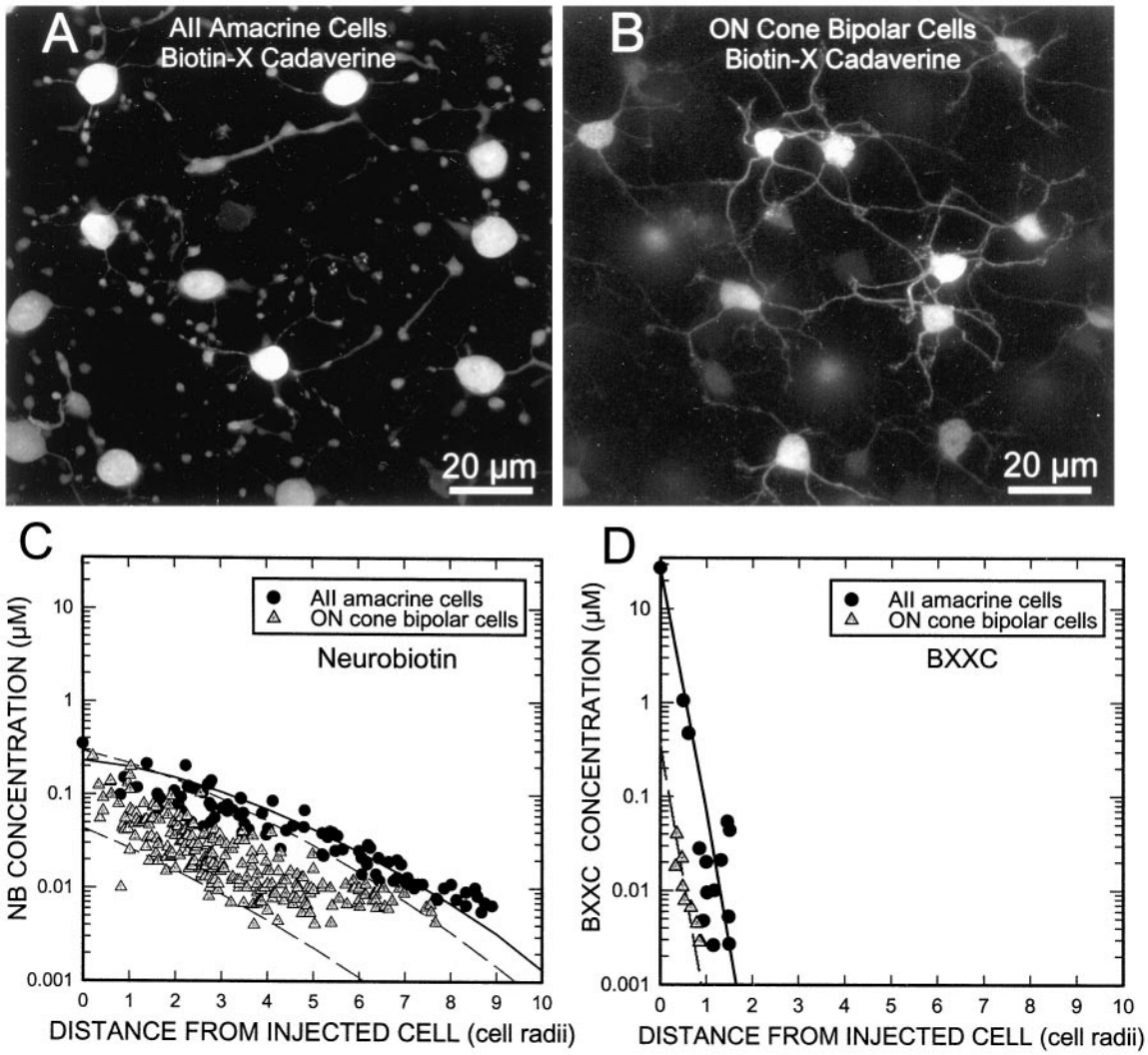

Figure 6. Coupling from injected AII amacrine cells to other AII amacrines and ON cone bipolar cells. *A*, Biotin-X cadaverine injected into a single AII has stained many nearby AII amacrine cells, easily distinguished by their lobules in sublamina a of the inner plexiform layer. *B*, BXC from the same injection also stained some ON cone bipolar cells, whose dendrites are seen ramifying in the outer plexiform layer. These two confocal micrographs consist of stacks of 0.5 μm sections. *C*, Another AII amacrine cell injected with Neurobiotin (*NB*) shows the decline in fluorescent intensity across the mosaic of coupled AII amacrine cell somas (*black circles*), as well as ON cone bipolar cells (*gray triangles*). The *solid black line* is the best fit to the AII–AII coupling rate using the diffusion model. The *gray dashed lines* model the range of AII–bipolar cell rate constants. *D*, Staining of the AII mosaic declined more rapidly if BXXC is the tracer. The ON cone bipolar cell staining was reduced by an even greater factor. The single *gray dashed line* shows the coupling rate from the AII amacrine cells to the sparser population of coupled bipolar cells, which are stained with BXXC.

The slopes of the permeability × size profiles of the five gap junctional pathways were significantly different ($F_{(4)} = 261.5$; $p < 0.0001$). The specific results were as follows. (1) The decline in permeability with size of A-type horizontal cells gap junctions was significantly less than that of all other groups ($t = 5.5$; $p < 0.001$). (2) The permeability profiles of the gap junctions interconnecting B-type horizontal cells, AII-to-AII amacrine cells, and S1-to-S1 amacrine cells were not significantly different from one another ($t = 0.15–0.48$; $p > 0.1$). (3) The permeability of the gap junctions connecting ON cone bipolar cells to AII amacrine cells fell significantly more rapidly than between horizontal cells or pairs of AII amacrine cells ($t = 1.97–5.50$; $p < 0.05$). The differences between the AII–ON cone bipolar cell gap junctional pathways and the S1–S1 pathway was nonsignificant ($t = 1.42$; $p = 0.15$). We therefore conclude that at least three functionally different channel types, that is, with discriminable permeabilities, are expressed in rabbit retina. The most direct interpretation is that at least three different connexin types are represented, although three different modifications of a single type or three different mixtures of two types could also explain the results.

Possible changes in permeability states

There are at least two alternative interpretations that question whether the gap junctions behave as if they had a single dominant conductance state. (1) Gap junctional plaques could consist of channels made up of different connexin proteins in different proportions. This could produce differences in permeability with increasing tracer size across cell types. If this were true, it would nevertheless be surprising if the different connexin types were gated identically when exposed to substances that altered their open probabilities. (2) A second possibility is that channels consist of only a single connexin type in both cell types but with different active subconductance states. It might then be possible to shift between the states with the proper modulators.

The dye series can also be used to test these interpretations. If a modulator alters either the relative open probabilities of discriminably different connexon types or the distribution of conductance states of a single connexon type, the result would be a shift in permeability with the size of tracer relative to control conditions. We therefore injected tracers into A-type horizontal cells whose gap junctional permeability was reduced via two different agents.

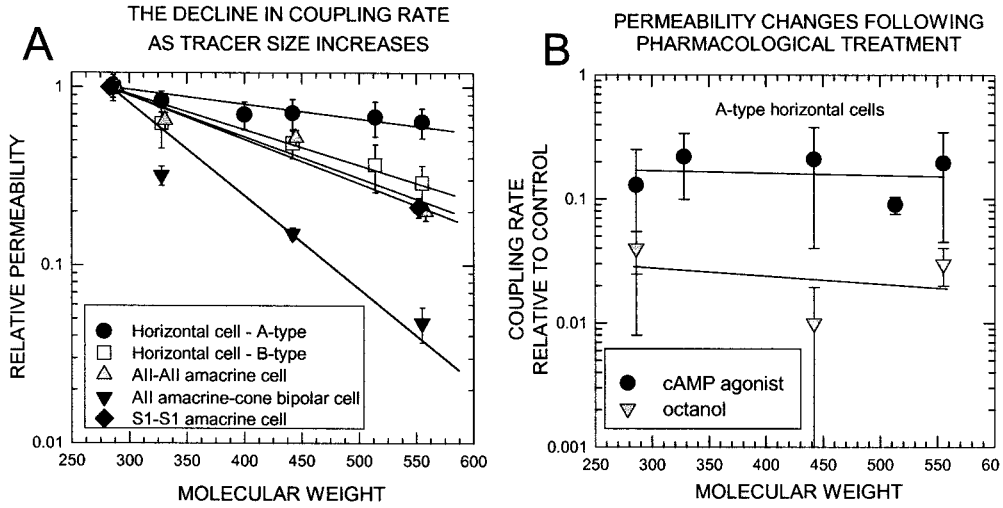

Figure 7. *A*, The ratio of permeabilities of each tracer relative to Neurobiotin was different for A-type horizontal cells (*circles*) than for other cell types (B-type horizontal cells, *triangles*; AII amacrine cell-to-AII amacrine cell, *squares*; S1 amacrine cells, *inverted triangles*). *Lines* are least squares fits from SigmaPlot (SPSS Inc., Chicago, IL). The decline was even greater for the presumed heterotypic gap junctions between AII amacrine cells and ON cone bipolar cells (*triangles*). Number of cells injected, in order of increasing tracer size: A-type horizontal cells, 23, 7, 5, 14, 8, 16; B-type horizontal cells, 21, 5, 0, 13, 5, 9; AII amacrine cells (to AII or bipolar cells), 20, 5, 0, 15, 0, 6; S1 amacrine cells, 4, 0, 0, 0, 0, 3. To facilitate inspection of SE bars, some points are displaced ±3 Da on the abscissa. *B*, In A-type horizontal cells, the ratio of permeabilities of pharmacological gating compounds to the control was constant across tracers. The effect of the cAMP agonist Sp-8-CPT-cAMPS (10 μM; *circles*) was as if mean open time was reduced to 10% of control; octanol (1 mM; *triangles*) reduced mean open time to 2% of control. The horizontal slope implies there was no change in fundamental connexon permeabilities induced by these substances over this range of molecular weights, although total permeability was dramatically reduced.

Figure 7*B* shows the ratio of permeabilities reduced by the modulators relative to controls without modulator. Octanol (1 mM), a nonspecific gap junctional modulator, lowered permeability to Neurobiotin 50-fold (Fig. 7*B*, *circles*). Elevations in cAMP have also been shown to close A-type horizontal cell gap junctions (Hampson et al., 1994). The potent cAMP analog Sp-8-CPT-cAMPS (10 μM) lowered Neurobiotin permeability 10-fold (Fig. 7*B*, *inverted triangles*). However, neither octanol nor the cAMP analog produced any decline in the permeability relative to Neurobiotin as tracer size increased. The least squares regression to the points did not significantly differ from a line with a slope of 0 ($t < 0.5$; $p > 0.1$). Therefore, the decline in permeability in each case was not caused by a shift to a less conductive state for the individual channels or a shift in relative open time of different channels. The parallel functions indicate that, over the span of the series, the only change induced by the modulators was a decline in open probability. Changes in subconductance states too small for Neurobiotin to pass cannot be excluded. The finding that putative channel closing agents reduce total permeabilities but do not alter relative permeability of tracers also serves to validate the procedure.

Tracers can be chosen to optimize staining of particular neuronal details

Another advantage of having a series of tracers is that the choice of tracer can be tailored to the properties of the preparation to produce a revealing result. When Neurobiotin is injected into B-type horizontal cells, the somas and dendrites are well stained. The long, thin axon, however, has a high impedance relative to the somatic gap junctions. Although the axon terminals can be stained with Neurobiotin under some conditions (Vaney, 1993), the quality of staining increases with increasing tracer size. BXXC, the largest tracer, is less likely to pass through somatic gap junctions and thereby stains the profuse axonal arbor in detail, also revealing the gap junctions between the axon terminals. This is shown in Figure 4, *B* and *D*. Figure 4*D* also illustrates the coupling between B-type horizontal cell axon terminals (Vaney, 1993; Bloomfield et al., 1995) and that these gap junctional connexons are also permeant to our largest tracer.

Even in less elaborate mosaics, such as the A-type horizontal cell, Neurobiotin often produces incomplete staining of fine dendritic detail, because the concentration rapidly drops as a result of large flux through the gap junctions. Larger tracers such as BXXC produce larger final concentrations of tracer in the injected cell and its near neighbors, resulting in superior staining of the fine processes.

DISCUSSION

We have used a series of structurally related tracers to determine several important features about retinal gap junctions. The permeabilities of the channels examined thus far fall into three distinct groups. We conclude, therefore, that at least three functionally different types of gap junctional channel are represented in the neural retina.

Possible mechanisms of permeability differences

The most direct interpretation of our results is that the retina contains at least three different neural connexins, but there are several alternative explanations for the permeability differences. These include the following: (1) different post-translational modifications of a single connexin type, (2) activation of different subconductance states of a single multiple-conductance channel, or (3) different proportions of multiple connexin types with different permeability characteristics. The modulation experiments (Fig. 7*B*) argue against the last possibility.

Two or more connexin types could occur in gap junctional plaques that contain homotypic connexons (each channel consists entirely of one connexin type) or are heterotypic (the hemichannels are each of a single connexin type but are different from each other) or heteromeric (the hemichannels themselves are comprised of mixed connexin types). The tracer series cannot distinguish among these possibilities but can indicate whether two gap junctional networks are discriminably different in their average permeability. Our goal here is not the identification of specific connexin types, which cannot be done by tracer injection, but the detection of functional differences in gap junctions at different sites in intact neural tissue. The results suggest that several neuronal connexins remain to be identified.

Tracer coupling and electrical coupling

It is unclear whether relative degrees of electrical coupling closely mirror the relative permeabilities in these circuits. Conductances of small current-carrying ions could be sensitive to conductance

states not sampled by the larger molecules and that could be modulated differentially from the large permeability states (Kwak et al., 1995). In the retinal horizontal cell networks, however, the relative ratios of Neurobiotin permeability are of the same magnitude as their relative electrical coupling (Bloomfield et al., 1995; Mills and Massey, 1998). The tracer series is useful in distinguishing whether modulators shift permeability states within the permeability range of the series but must be extrapolated with caution.

The potential diversity of neuronal connexins

The identification of neuronal gap junctions with characterized connexins is only recently beginning to show success. O'Brien et al. (1996) and Condorelli et al. (1998) have identified a novel connexin type (Cx35 or the mammalian homolog Cx36) in retina and brain. Srinivas et al. (1999) showed that channels formed from Cx36 had the lowest conductance of any presently identified connexin but surprisingly seemed to pass Lucifer yellow. Only A-type horizontal cells typically show Lucifer yellow coupling in rabbit retina. Preliminary evidence suggests that Cx36 is associated with AII amacrine cells in rat and rabbit retina (O'Brien et al., 2000; Weiler et al., 2000) and that horizontal cells are not labeled by Cx36 immunostaining.

Why might there be several different types of connexin within a single type of tissue? Neural tissue consists of many distinctly different cell types, often in close proximity. Different connexin types could prevent gap junctions from forming between cell types that need to remain distinct. A- and B-type horizontal cells, which share similar functions but maintain different receptive field sizes, are an example of neighboring neurons that should not couple to one another. Conversely, different cells that are capable of forming heterotypic gap junctions enable differential regulation of permeability from the opposite sides of the channel. AII amacrine cells are a likely example (Mills and Massey, 1995) Finally, recent evidence suggests that channels made of different connexin types can differentially pass second messengers (Bevans et al., 1998; Goldberg et al., 1999; Niessen et al., 2000). Messengers with a negative charge, such as the cyclic nucleotides and inositol 1,4,5-triphosphate, are unlikely to freely pass channels impermeant to Lucifer yellow. In this study, that would include all but those in A-type horizontal cells. Calcium ions should not be restricted on the basis of charge, although they might alter channel gating.

Use of the series

A strength of this series is that all six tracers are visualized by the same mechanism, the binding of streptavidin-Cy3 to the biotin moiety. Each tracer therefore has identical excitation and emission bands, extinction coefficients, and photobleaching rates when visualized. Each member of the biotinylated series also bears the same net charge (+1), although the surface charge distribution may vary (Veenstra et al., 1994). One might presume that they also share the same detection efficiency, but some increased affinity of longer tracers has been found (Fig. 2) (Hofmann et al., 1982; Haugland and You, 1995).

This tracer series has many other good properties. Its members are readily water-soluble, fixable, relatively nonreactive, membrane-impermeant, differ mostly in size, and are cationic, matching the permeability preferences of many connexon types. Our results demonstrate the usefulness of this series in assaying gap junctional permeability. It is especially applicable *in vivo* in which other methods are difficult. Finally, measuring the flux of these medium-sized molecules in intact systems may facilitate comparison with physiologically important second-messenger systems (Saez et al., 1989; Goldberg et al., 1999; Niessen et al., 2000).

It is not necessary to use all six members of the series to determine whether two gap junctional pathways are discriminably different, although we often used most or all members to validate the method. In fact, adequate sampling of a single pair of tracers can be sufficient (Zimmerman and Rose, 1985; Mills and Massey, 1995).

This report is the first to systematically examine the physiological diversity of gap junctions in neural tissue and provides evidence for multiple different gap junctional units in the retina. The diversity found at chemical synapses has recently become apparent. It is not surprising that electrical synapses might be similarly diverse.

REFERENCES

Bevans CG, Kordel M, Rhee SK, Harris AL (1998) Isoform composition of connexin channels determines selectivity among second messengers and uncharged molecules. J Biol Chem 273:2808–2816.

Bloomfield SA, Xin D, Persky SE (1995) A comparison of receptive field and tracer coupling size of horizontal cells in the rabbit retina. Vis Neurosci 12:985–999.

Brink PR, Dewey MM (1978) Nexal membrane permeability to anions. J Gen Physiol 72:67–86.

Brink PR, Dewey MM (1980) Evidence for fixed charge in the nexus. Nature 285:101–102.

Bruzzone R, White TW, Paul DL (1994) Expression of chimeric connexins reveals new properties of the formation and gating behavior of gap junction channels. J Cell Sci 107:955–967.

Cao F, Eckert R, Elfgang C, Mitsche JM, Snyder SA, Hülser DF, Willecke K Nicholson BF (1998) A quantitative analysis of connexin-specific permeability differences of gap junctions expressed in HeLa transfectants and *Xenopus* oocytes. J Cell Sci 111:31–43.

Condorelli DF, Parenti R, Spinella F, Trovato Salinaro A, Belluardo N, Cardile V, Ciciata F (1998) Cloning of a new gap junction gene (Cx36) highly expressed in mammalian brain neurons. Eur J Neurosci 10:1202–1208.

Dacheux RF, Raviola E (1982) Horizontal cells in the retina of the rabbit. J Neurosci 2:1486–1493.

Flagg-Newton J, Simpson I, Loewenstein WR (1979) Permeability of the cell-to-cell membrane channels in mammalian cell junction. Science 205:404–407.

Goldberg GS, Lampe PD, Nicholson BJ (1999) Selective transfer of endogenous metabolites through gap junctions composed of different connexins. Nat Cell Biol 1:457–459.

Hampson ECGM, Weiler R, Vaney DI (1994) pH-gated dopaminergic modulation of horizontal cell gap junctions in mammalian retina. Proc R Soc Lond B Biol Sci 255:67–72.

Haugland RP, You WW (1995) Coupling of monoclonal antibodies with biotin. Methods Mol Biol 45:223–233.

Hofmann K, Titus G, Montibeller JA, Finn FM (1982) Avidin binding of carboxyl-substituted biotin and analogues. Biochemistry 21:978–984.

Iminaga I (1989) Cell-to-cell diffusion of large molecules in cardiac cells. In: Cell interactions and gap junctions, Vol II (Sperelakis N, Cole WC, eds), pp 49–63. Boca Raton, FL: CRC.

Kwak BR, van Veen TAB, Analber LJS, Jongsma HJ (1995) TPA increases conductance but decreases permeability in neonatal rat cardiomyocyte gap junction channels. Exp Cell Res 200:456–463.

Mills SL, Massey SC (1994) Distribution and coverage of A- and B-type horizontal cells stained with Neurobiotin in the rabbit retina. Vis Neurosci 11:549–560.

Mills SL, Massey SC (1995) Differential properties of two gap junctional pathways made by AII amacrine cells. Nature 377:734–737.

Mills SL, Massey SC (1998) The kinetics of tracer movement through homologous retinal gap junctions. Vis Neurosci 15:765–777.

Niessen H, Harz H, Bedner P, Kämer K, Willecke K (2000) Selective permeability of different connexin channels to the second messenger inositol 1,4,5-triphosphate. J Cell Sci 113:1365–1372.

O'Brien J, al-Ubaidi MR, Ripps H (1996) Connexin35: a gap-junctional protein expressed preferentially in the skate retina. Mol Biol Cell 7:233–243.

O'Brien JJ, Mills SL, O'Brien J, Li W, Massey SC (2000) Confocal analysis of connexin36-immunoreactivity in rabbit retina. Soc Neurosci Abstr 26:662.

Saez JC, Connor JA, Spray DC, Bennett MV (1989) Hepatocyte gap junctions are permeable to the second messenger, inositol 1,4,5-trisphosphate, and to calcium ions. Proc Natl Acad Sci USA 86:2708–2712.

Schwarzmann G, Wiegandt H, Rose B, Zimmerman A, Ben-Haim D, Loewenstein WR (1981) Diameter of the cell-to-cell junctional membrane channels as probed with neutral molecules. Science 213:552–553.

Srinivas M, Rozental R, Kojima T, Dermietzel R, Mehler M, Condorelli DF, Kessler JA, Spray DC (1999) Functional properties of channels formed by the neuronal gap junction protein connexin36. J Neurosci 19:9848–9855.

Strettoi E, Dacheux RF, Ravioa E (1990) Synaptic connections of rod bipolar cells in the inner plexiform layer of the rabbit retina. J Comp Neurol 295:449–466.

Swenson KL, Jordan JR, Beyer EC, Paul DL (1989) Formation of gap junctions by expression of connexins in *Xenopus* oocyte pairs. Cell 57:145–155.
Vaney DI (1991) Many diverse types of retinal neurons show tracer coupling when injected with biocytin or Neurobiotin. J Neurosci Lett 125:187–190.
Vaney DI (1993) The coupling pattern of axon-bearing horizontal cells in the mammalian retina. Proc R Soc Lond B Biol Sci 252:93–101.
Vaney DI (1999) Neuronal coupling in the central nervous system: lessons from the retina. Novartis Found Symp 219:113–125.
Veenstra RD, Wang H-Z, Beyer EC, Brink PR (1994) Selective dye and ionic permeability of gap junction channels formed by connexin45. Circ Res 75:483–490.
Veenstra RD, Wang H-Z, Beblo DA, Chilton MG, Harris AL, Beyer EC, Brink PR (1995) Selectivity of connexin-specific gap junctions does not correlate with channel conductance. Circ Res 77: 1156–1165.
Weiler R, Feigenspan A, Teubner B, Willecke K (2000) Cellular localization of the murine connexin Cx36 in the mammalian retina. Invest Ophthamol Vis Sci [Suppl] 41:S620.
Werner R, Levine E, Rabadan-Diehl C, Dahl G (1989) Formation of hybrid cell-cell channels. Proc Natl Acad Sci USA 86:5380–5384.
Zimmerman AL, Rose B (1985) Permeability properties of cell-to-cell channels: kinetics of fluorescent tracer diffusion through a cell junction. J Membr Biol 84:269–283.